FUDMA Journal of Sciences (FJS)
ISSN online: 2616-1370
ISSN print: 2645 - 2944
Vol. 10 No. 4, February, 2026, pp 236 – 247
DOI: https://doi.org/10.33003/fjs-2026-1004-4884

ANALYSIS OF RADIATION SHIELDING PARAMETERS OF PRISTINE AND GADOLINIUM OXIDE DOPED ZINC BOROTELLURITE GLASS SYSTEM

[1]Reuben Abraham Solomon and [2]Oluwatosin Mary Kayode

[1]Department of Physics, Bayero University Kano, Kano State, Nigeria.
[2]Department of Science Education, Ibrahim Badamasi University, Lapai, Niger State, Nigeria.

*Corresponding Auhtor's Email: solomonreuben1010@gmail.com

ABSTRACT

Convectional radiation shielding materials such as lead and concrete present significant toxicity and structural limitations, underscoring the need for safe, high performance glass based alternatives. This paper studies the radiation shielding parameter for the glass of Gd_2O_3-doped zinc borotellurite glasses, with varying concentrations of Gd_2O_3 (x = 0.0 to 0.05 mol, coded as S1 to S6). Theoretical calculations using Phy-X and WinXCom software reveal that the glass sample with 5% Gd_2O_3 (S6) exhibits superior radiation shielding performance, with the highest mass attenuation coefficient (MAC = 0.07623 cm2/g at 0.662 MeV), linear attenuation coefficient (LAC) and effective atomic number (Z_{eff} = 19.10 at 0.662 MeV), as well as the lowest half-value layer (HVL = 1.857 cm at 0.662 MeV) and mean free path (MFP = 2.679 cm at 0.662 MeV) values. The results show a direct correlation between the concentration of Gd_2O_3 and the material's radiation shielding properties, with S6 demonstrating the best performance. Comparison with lead-free and concrete radiation shielding materials for gamma energies 0.662 MeV, 1.17 MeV and 1.332 MeV reveals that S6 outperforms all compared materials in HVL, MFP and Z_{eff}, highlighting its potential as a superior radiation shielding material. The maximum deviation between MAC value calculated via Phy-X and WinXCom results is 0.088%, confirming the reliability of the calculations.

Keywords: Density, Lead-free glass, Radiation shielding properties, Gamma-rays, Mass attenuation coefficient

INTRODUCTION

In today's world, glass has become indispensable material in modern life, distinguished by its unique amorphous structure that sets it apart from other solids (Callister & Rethwisch 2011; Hasnimulyati *et al*., 2021). Glass ability to effectively transmit light has made it a vital material in diverse applications, including photonics, electronics and communications, radiation shielding and other fields. The growing utilization of glass in radiation shielding applications, especially in medical treatment has intensify the need to quantify the shielding ability of this materials (Echeweozo *et al*., 2025). This worry is as a result of the emergence of the radiological effects linked to the interaction between radiation and glass (Saheb *et al*., 2018). The biological risk associated with ionizing radiation include DNA strand breaks, increased carcinogenesis risk, and acute radiation syndrome directly motivate the engineering of superior shielding materials that reduce effective dose in medical and nuclear environments (Saheb, et al., 2018).

Protecting the population from radiation's hazardous effects is crucial. It's vital to prioritize studies on protective measures and materials to safeguard public health. Investigating the radiation attenuation properties of various materials is key to developing efficient radiation shielding solutions (Hatice, 2024). Lead consisting glasses are still being used for medical and industrial purposes owing to their mechanical durability that is high resistance to corrosion, high atomic number, degradation over time, availability and cost (Rusni *et al.*, 2024). Lead due to its toxicity, it exposure can have devastating effects on human health, particularly children. A recent investigation in two villages in Zamfara State, Nigeria, found alarming levels of lead in homes, water, and children's blood, resulting in significant mortality rates (of one-fourth of children in the past year) (Udiba *et al.*, 2019). This highlights the importance of controlling the exposure and exploring alternative materials, such as lead free glasses to mitigate this risk. Concrete, another common shielding significant thickness and degrade over time. Although various study have explored radiation shielding properties of lead-free materials, there remains a need to investigate and compare the radiation attenuation characteristics of lead-free glasses with those of traditional lead-based glasses. To address these issue, there is a need to study pristine and gadolinium doped zinc borotellurite glass composition, leveraging on gadolinium's high density, high atomic number and chemical stability, to provide a safer and more efficient alternative.

Gadolinium oxide, Gd_2O_3 known for its promising component material for photonics and optoelectronics application (Eevon *et al.*, 2016). This study proposes a novel glass composition incorporating Gd_2O_3, and tellurium dioxide (TeO_2) to enhance elastic, thermal stability and chemical durability. The addition of boron oxide (B_2O_3) and zinc oxide (ZnO), improves the glass's properties, including its high density (4.896g/cm^3), hardness, and chemical durability, making it a promising material for radiation shielding (Eevon, M, Z, & C, 2016). The glass composition, $\{[(TeO_2)_{0.7}(B_2O_3)_{0.3}]_{0.7}[ZnO]_{0.3}\}_{1-x}\{Gd_2O_3\}_x$ (where x= 0.0, 0.01, 0.02, 0.03,0.04 and 0.05), combines the benefit of tellurite and borate glasses, including non-toxicity, cost-effectiveness and high bond strength with oxygen (Sayyed, 2021; Matori *et al*., 2017; Teresa *et al.*, 2021). The incorporation of ZnO enhances the glass's properties, acting as both modifier and network former (Al-Hadeethi *et al.*, 2020; El-Mallawany, 2002). The addition of ZnO enhances the glass's linear attenuation coefficient (LAC) and density (Effendy *et al*., 2021). Gadolinium environmental safety profile and potential for radiation shielding applications warrant further research. However, there is still lack of systematic study on zinc borotellurite radiation shielding glass doped with gadolinium oxide specifically, the quantitative relationship between G2O3 concentration (0-5%) and the full suite of shielding parameters across the broad photon energy spectrum relevant to medical and industrial applications has not been systematically reported.

The aim of this study is to analyze radiation shielding parameters and explores the effects of different energies of gamma rays-radiation shielding properties on gadolinium-doped zinc borotellurite glass building on previous work by Eevon *et al* (2016) and then compare them with existing research. The estimated parameters including mass attenuation coefficient (MAC), linear attenuation coefficient (LAC), half value layer (HVL), mean free path (MFP) and effective atomic number (Z_{eff}). This study also compare these parameters using Phy-X/PSD and WinXCOM software programs. Hence, this research can contribute to existing body of information for future applications.

MATERIALS AND METHODS

Chemical and Instrumentation

The Phy-X/PSD and WinXCOM software were employed to compute some gamma-ray attenuation properties of pure and gadolinium oxide doped borotellurite glasses with the empirical formula $\{[(TeO_2)_{0.7}(B_2O_3)_{0.3}]_{0.7}[ZnO]_{0.3}\}_{1-x}\{Gd_2O_3\}_x$ with $x = 0.01, 0.02, 0.03, 0.04$ *and* 0.05 mol.

Glass Preparation

The glasses prepared by Eevon *et al.*, (2016) via conventional melt-quenching method with composition, average molecular weight and density as shown in Table 1 and Figure 1 were used in this study. The glasses were coded as S1, S2, S3, S4, S5 and S6 which correspond to 0%, 1%, 2%, 3%, 4% and 5mol % of Gd_2O_3 respectively.

Phy-X/PSD Software

Phy-X/PSD software was developed by Erdem *et al* (2019) with the aim of calculating parameters that are relevant to radiation shielding parameters. In this work, Phy-X/PSD software was employed to compute the radiation shielding parameters of various gadolinium doped borotellurite glass. Calculation process commenced by defining the material composition and the corresponding density of the given materials in the software. Calculation was done via mole ratio of the constituent compound in each mixture. The energy range was set to 0.001 MeV – 10^5 MeV and gamma radiation sources ^{137}Cs and ^{60}Co were selected to include specific calculations for photon energies 0.662 MeV, 1.17 MeV and 1.332 MeV. These energies represent typical gamma spectra encounter in real operational conditions such as hospitals, nuclear research centres and industrial radiation facilities The output parameters selected include Atomic Mass Weight (AMW), Mass Attenuation Coefficient (MAC), Linear Attenuation Coefficient (LAC), Half-Value Layer (HVL), Mean Free Path (MFP) and Effective Attenuation Number (Z_{eff}). After calculation, the result were generated and download to Microsoft Excel for further analysis and graphing.

WinXCOM

For the WinXCOM software, the material was defined as mixture, and the weight fraction was fraction of each compound in a given material was calculated using equation (8). The compounds and their corresponding weight fractions were entered into the WinXCOM interface, and the energy range was set to 0.001 MeV and 10^5 MeV. Additional energies (0.662 MeV, 1.17 MeV and 1.332 MeV) were also included for calculations. The software output the Mass Attenuation coefficient (MAC) for the specified energy range. Unlike Phy-X/PSD, which directly calculates multiple parameters, XCOM only output MAC values. These values were then downloaded to Microsoft Excel, were further calculations were then performed using equations 2-7 to determine other shielding parameters, such as, Linear Attenuation Coefficient (LAC), Half-Value Layer (HVL), Mean Free Path (MFP) and Effective Attenuation Number (Z_{eff}). The result were then plotted and analyzed. The aim of using the XCOM software is to validate the result obtained from Phy-X/PSD software (Berger & Hubbell, 1987).

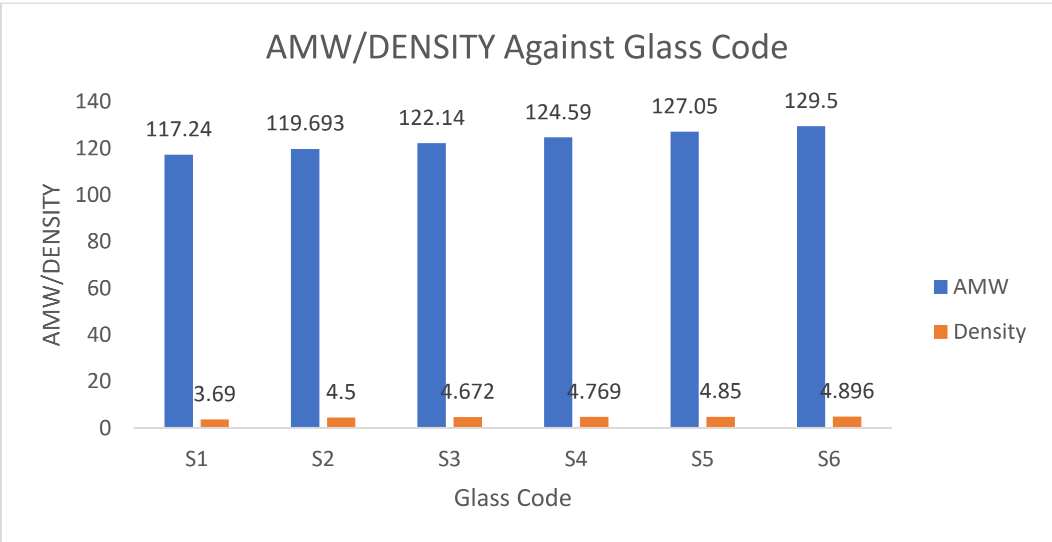

Figure 1: Average Molecular Weight (AMW) in g/mol and Density (ρ) gcm^{-3} Versus Glass Code

Table 1: Chemical Composition of $\{[(TeO_2)_{0.7}(B_2O_3)_{0.3}]_{0.7}[ZnO]_{0.3}\}_{1-x}\{Gd_2O_3\}_x$ Glass System for Different Concentrations of Gd_2O_3 and Corresponding Densities

Glass Code	Gd_2O_3 (mol%)	Glass Composition	Density (g/cm^{3})
S1	0	$\{[(TeO_2)_{0.7}(B_2O_3)_{0.3}]_{0.7}[ZnO]_{0.3}\}_{1-x}\{Gd_2O_3\}_x$	3.690
S2	1	$\{[(TeO_2)_{0.7}(B_2O_3)_{0.3}]_{0.7}[ZnO]_{0.3}\}_{1-x}\{Gd_2O_3\}_x$	4.500
S3	2	$\{[(TeO_2)_{0.7}(B_2O_3)_{0.3}]_{0.7}[ZnO]_{0.3}\}_{1-x}\{Gd_2O_3\}_x$	4.672

Glass Code	Gd_2O_3 (mol%)	Glass Composition	Density (g/cm$^{3)}$
S4	3	$\{[(TeO_2)_{0.7}(B_2O_3)_{0.3}]_{0.7}[ZnO]_{0.3}\}_{1-x}\{Gd_2O_3\}_x$	4.769
S5	4	$\{[(TeO_2)_{0.7}(B_2O_3)_{0.3}]_{0.7}[ZnO]_{0.3}\}_{1-x}\{Gd_2O_3\}_x$	4.850
S6	5	$\{[(TeO_2)_{0.7}(B_2O_3)_{0.3}]_{0.7}[ZnO]_{0.3}\}_{1-x}\{Gd_2O_3\}_x$	4.896

Shielding

Shielding Parameter Calculation

The shielding parameters such as the mass attenuation coefficient (MAC), linear attenuation coefficient (LAC), half value layer (HVL), mean free path (MFP), effective atomic number (Z_{eff}) for given energies can be obtained directly through Phy-x/PSD software, while WinXCOM only output the MAC value for the assign photon energies which can then be used to calculate the required shielding parameters. To employ mixture rule and exponential attenuation law, each material under investigation is completely homogeneous mixture. However, real glass microstructure, phase heterogeneity and elemental clustering could locally modify attenuation properties.

The formula for determining LAC is given by (Al-Hadeethi *et al*., 2020)

$$LAC = MAC\ X\ \rho \qquad (1)$$

where ρ is the density of the material in g/cm^3. The units of MAC and LAC are cm^2/g and cm^{-1} respectively

From the LAC value(s) the HVL with the unit (cm) can be obtained using equation (2) (Al-Hadeethi *et al.,* 2020)

$$HVL = \frac{0.693}{LAC} \qquad (2)$$

The obtained value of LAC can also be used in (3) to calculate TVL (Jamal *et al*., 2020)

$$TVL = \frac{2.303}{LAC} \qquad (3)$$

MFP is the reciprocal of LAC and may be determine using (Ozpolat *et al*., 2020; Sayyed, 2021)

$$MFP = \frac{1}{LAC} \qquad (4)$$

MAC and ACS are related by the relation (Teresa, *et al*., 2021)

$$ACS = \frac{MAC}{N_A \sum \frac{W}{A}} \qquad (5)$$

Where N_A, is the avogradro's number, A is the atomic weight constituent element, and w is the weight fraction of each element. Thus ECS, is also related to MAC via the formula (Azuraida, 2018)

$$ECS = \frac{1}{N_A}\left(\sum \frac{f.A}{Z}.(MAC)\right) \qquad (6)$$

In the above equation $f, Z\ and\ Z_{eff}$ are the fractional abundance of element, atomic number of element and effective number respectively. Z_{eff} Can be found via ACS and ECS using the ration (Azuraida, 2018)

$$Z_{eff} = \frac{ACS}{ECS} \qquad (7)$$

The weight faction of individual element w in (5) is obtained using (Azuraida, 2018)

$$w = \frac{n \cdot A}{\sum n \cdot A} \qquad (8)$$

The deviation ΔS_I (for I = 1, 2, 3, ……,6) of shielding parameter for the samples obtained between Phy-X and WinXCOM was calculated using the equation (Kavaz, et al., 2019; Singh, Kaur, Rani, Sidhu, & S, 2021)

$$\Delta S_I = \frac{|Result_{Phy-X} - Result_{XCOM}|}{Result_{Phy-X}} \times 100\% \qquad (9)$$

RESULTS AND DISCUSSION

Mass Attenuation Coefficient (MAC)

MAC describes how strongly a material interacts with radiation, independent of its density. All other shielding parameters depend on MAC. The higher the MAC, the more effectively a material attenuates, absorbs or scatters radiation. In this study, the MAC values calculated using Phy-X/PSD and WinXCOM software (see Tables 2 and 3) exhibit strong consistency, indicating good agreement with each other. This consistency of MAC values calculated by the two software is further confirmed by the small deviations presented in Table 4, with a maximum deviation of 0.088%. This discrepancy validates the reliability of the calculations, demonstrating excellent agreement within the two softwares. For the pristine system, the calculated MAC value at 0.001 MeV is exactly 6001 cm^2/g with XCOM and 6000.827 cm^2/g with Phy-/PSD, which are in good agreement with previously reported value of 6001cm^2/g by (Rusni *et al*., 2024).

According to Tables 2 and 3, the MAC value increases with increase in the concentration of Gd_2O_3 content for photon energies between 0.001 MeV and 10^5 MeV. However, at 0.001 MeV, the MAC decreases with increasing Gd_2O_3 content. This suggests that the Gd doped glass samples are more effective for shielding radiation with energies above 0.01 MeV, making them suitable for gamma radiation shielding, since gamma rays typically have energies greater than 0.01 MeV (ARPANSA, 2022). Conversely, the pristine glass sample appears to be more effective for shielding X-rays, which typically have energies below 0.001 MeV, particularly the range where the MAC value is higher at 0.001 MeV. This makes the pristine glass a better choice for X-ray shielding applications.

Table 2: Mass Attenuation Coefficient of Pristine and Gd-doped Borotellurite Glass Calculated via Phy-X

Photon Energy (MeV)	S1	S2	S3	S4	S5	S6
0.001	6000.827	5897.696	5798.707	5703.615	5612.194	5524.236
0.01	120.654	124.100	127.407	130.584	133.638	136.576
0.1	1.089	1.139	1.186	1.232	1.275	1.317
1	0.05906	0.05914	0.05921	0.05928	0.05935	0.05941
10	0.03202	0.03229	0.03355	0.03279	0.03303	0.03325
100	0.04928	0.04995	0.0506	0.05122	0.05182	0.05239
1000	0.06049	0.06132	0.06212	0.063	0.06364	0.06436
10000	0.06294	0.06381	0.06464	0.06544	0.06621	0.06695
100000	0.06332	0.06419	0.06503	0.06583	0.06661	0.06736

Table 3: Mass Attenuation Coefficient of Pristine and Gd-doped Borotellurite Glass Calculated via WinXCOM

Photon Energy (MeV)	S1	S2	S3	S4	S5	S6
0.001	6001	5899	5801	5705	5610	5526
0.01	120.6	124.1	127.4	130.5	133.6	136.6
0.1	1.089	1.138	1.186	1.231	1.274	1.318
1	0.05906	0.05914	0.05921	0.05928	0.05935	0.05941
10	0.03202	0.03229	0.03255	0.03279	0.03302	0.03326
100	0.04927	0.04995	0.05061	0.05121	0.05179	0.05241
1000	0.06048	0.06131	0.06214	0.06289	0.06361	0.06437
10000	0.06293	0.0638	0.06465	0.06543	0.06618	0.06697
100000	0.06331	0.06418	0.06504	0.06582	0.06658	0.06738

Table 4: Deviation in MAC Calculated via Phy-X/PSD from WinXCOM

Photon Energy (MeV)	ΔS_1	ΔS_2	ΔS_3	ΔS_4	ΔS_5	ΔS_6
0.001	0.0029	0.022	0.04	0.024	0.039	0.032
0.01	0.045	0	0.0055	0.064	0.028	0.018
0.1	0	0.088	0	0.081	0.078	0.076
1	0	0	0	0	0	0
10	0	0	0	0	0.030	0.030
100	0.020	0	0.02	0.0195	0.0579	0.0381
1000	0.0165	0.0163	0.0322	0.0159	0.047	0.0133
10000	0.0159	0.0156	0.0155	0.0153	0.0151	0.0299
100000	0.0158	0.0156	0.0154	0.0152	0.045	0.0297

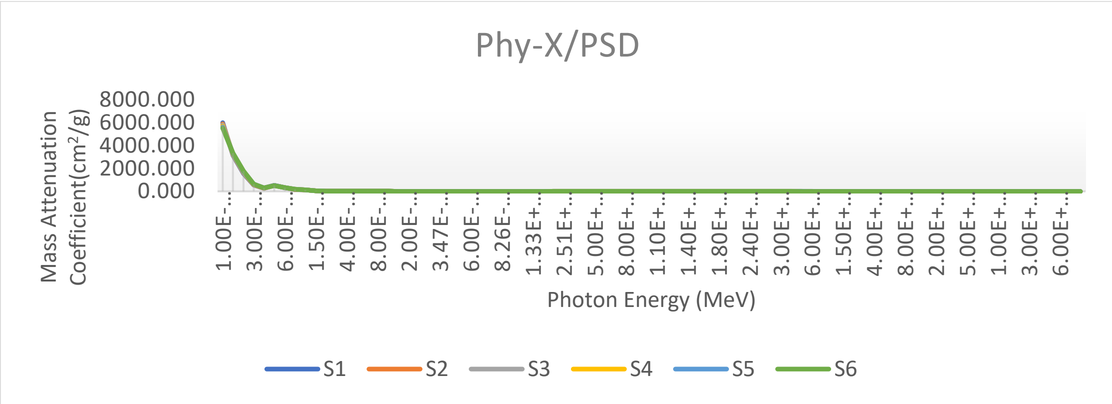

Figure 2: Mass Attenuation Coefficient of Pristine and Gd_2O_3 Doped-borotellurite Glass

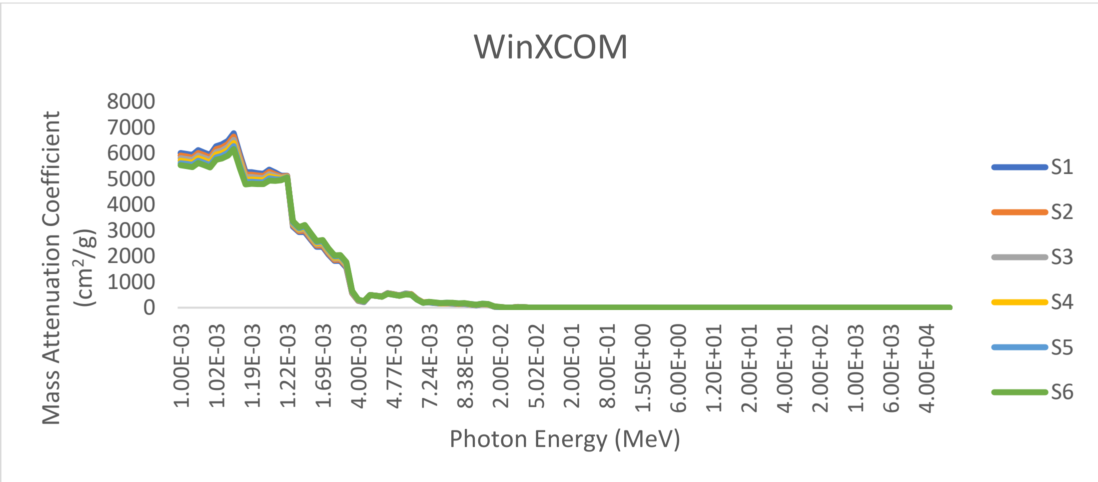

Figure 3: Mass Attenuation Coefficient of Pristine and Gd_2O_3 Doped-borotellurite Glass

Figures 2 and 3 compares the mass attenuation coefficients (MAC) of pristine and Gd_2O_3 doped zinc borotellurite glasses, calculated using Phy-X/PSD and WinXCOM software, across a wide photon energy range (10^{-3} to 10^5 MeV). The pristine sample (S1) corresponds to x = 0 in the composition $\{[(TeO_2)_{0.7}(B_2O_3)_{0.3}]_{0.7}[ZnO]_{0.3}\}_{1-x}\{Gd_2O_3\}_x$, while S2-S6 represent x =0.01, 0.02, 0.03, 0.04, 0.05 mol Gd_2O_3 respectively.

In both computational approaches, the MAC values exhibits a sharp decrease with increasing photon energy, which is characteristic of photon-matter interactions. At low photon energies ($\leq 0.1\ MeV$), with a cross-section that scale as

Z^4/E^3 as shown in Figures 2 and 3, the MAC is significantly higher due to dominance of the photoelectric absorption process, which is strongly dependent on the effective atomic number of the glass. The incorporation of Gd_2O_3, a high atomic number material ($Z = 64$), is expected to enhance the MAC in the region by increasing the average molecular weight, thereby improving the attenuation capability. However, the Phy-X/PSD output shows all compositions almost overlapping, likely due to limited numerical sensitivity or graphical scaling, whereas the WinXCOM results exhibits more pronounced variations between doped and undoped samples at low energies.

In the intermediate photon energy range ($\sim 0.1 - 1\ MeV$), where cross-section scale as $Z/_E$ for both Phy-x/PSD and WinXCOM, where Compton scattering predominates, MAC values become relatively energy-independent and differences between compositions diminish. This is consistent with the fact that Compton scattering probability depends weakly on Z and more on electron density. At higher energies ($> 1.022\ MeV$) with cross section scale as Z^4, pair production becomes significant, and a slight increase in MAC is observed for all samples, though the effect of doping remains minimal in this region (Teresa *et al*., 2021).

The comparison between Phy-X/PSD and WinXCOM reveals general agreement in the attenuation trends. WinXCOM provides a more detailed step like structure at low energies, reflecting the absorption edges of constituent elements, including gadolinium's K-edge ($\sim 50.2 keV$), which is less visible in the Phy-X/PSD results. These variations could be attributed to differences in the underlying cross-section databases and interpolation algorithms used by the two programs.

The Mass Attenuation Coefficient (MAC) results for gamma rays energies 0.662 MeV, 1.17 MeV and 1.332 MeV are presented in the below in the Tables 5 and 6 below . These gamma rays energies were selected due to their common applications in medicine (e.g radiotherapy), industry (sterilization and disinfection) and nuclear sectors (Kavaz *et al*., 2019; Roberts, 2003; Rusni *et al.*, 2004). According to Tables 5 and 6, the MAC increases with rising percentage of Gd_2O_3 in both software. At lower photon energies (0.662 MeV), XCOM result are generally slightly higher than those from Phy-X, whereas at higher energies (1.17 MeV and 1.332 MeV) Phy-X values surpass those of XCOM. This agrees with earlier report by (*Rusni et al.*, 2024), on Ce-doped zinc borotellurite glasses, where similar deviation trends are noted. Overall, Gd_2O_3 doping has the most notable impact at low energies, enhancing attenuation performance due to high-Z contribution of gadolinium. This suggests that Gd_2O_3-doped zinc borotellurite glasses could serve as effective gamma and X-ray shielding materials, particularly for applications involving low to medium photon energies. It is also found that the most promising candidate is 5% Gd_2O_3 content (S6), as it has the highest MAC and density. The strong agreement in general trends between the two computational tools confirm the reliability of the results, while the differences in fine details highlight the importance of cross-verifying data from multiple software platforms in radiation shielding research.

Table 5: Mass Attenuation Coefficient of Pure and Gd-doped Zinc Borotellurite Glass Calculated using Phy-X/PSD

Gamma rays Energy (MeV)	S1	S2	S3	S4	S5	S6
0.662	0.07492	0.0752	0.07547	0.07573	0.07598	0.07623
1.173	0.05406	0.05409	0.05413	0.05416	0.05419	0.05423
1.332	0.05049	0.05051	0.05054	0.05056	0.05058	0.0506

Table 6: Mass Attenuation Coefficient of Pristine and Gd-doped Borotellurite Glass Calculated using WinXCOM

Gamma rays Energy (MeV)	S1	S2	S3	S4	S5	S6
0.662	0.0749	0.07518	0.07545	0.07571	0.07596	0.0762
1.173	0.05413	0.05417	0.0542	0.05424	0.05428	0.0543
1.332	0.05051	0.05053	0.05056	0.05058	0.0506	0.05062

Linear Attenuation Coefficient (LAC)

The linear attenuation coefficient represents the probability of interaction between the radiation and the material per unit path length. The higher the LAC value, the more effectively the material reduces the intensity of radiation as it pass through. This study examined the gamma-ray attenuation properties of pristine and Gd_2O_3- doped zinc borotelurite glass with results presented in Tables 7 and 8. These Tables shows that the LAC value increases as the concentration of the dopant (Gd_2O_3) increases. This increment in LAC value can be ascribe to increasing molecular weight of the compound as well as the density.

Table 7: Linear Attenuation Coefficient of Pristine and Gd-doped Borotellurite Glass Calculated via Phy-X/PSD

Photon Energy (MeV)	S1	S2	S3	S4	S5	S6
0.001	22143.051	26539.633	27091.560	27200.541	27219.143	27046.661
0.01	445.215	558.449	595.245	622.754	648.144	668.678
0.1	4.020	5.124	5.542	5.874	6.185	6.450
1	0.218	0.266	0.277	0.283	0.288	0.291
10	0.1182	0.1453	0.1521	0.1564	0.1602	0.1628
100	0.1818	0.2248	0.2364	0.2443	0.2513	0.2565
1000	0.2232	0.2760	0.2903	0.300	0.3087	0.3151
10000	0.2322	0.2871	0.3019	0.3121	0.3211	0.3278
100000	0.2336	0.2889	0.3038	0.314	0.3231	0.3298

Table 8: Linear Attenuation Coefficient of Pristine and Gd-doped Borotellurite Glass Calculated via WinXCOM

Photon Energy (MeV)	S1	S2	S3	S4	S5	S6
0.001	22143.69	26545.5	27102.272	27207.15	27208.5	27055.3
0.01	445.014	558.450	595.2128	622.3545	647.96	668.7936
0.1	4.01841	5.1210	5.540992	5.870639	6.1789	6.452928
1	0.217931	0.26613	0.27662912	0.282706	0.287848	0.290871
10	0.118154	0.145305	0.1520736	0.156376	0.160147	0.164897
100	0.181806	0.224775	0.23644992	0.24422	0.251182	0.256599
1000	0.223171	0.275895	0.29031808	0.299922	0.308509	0.315156
10000	0.232212	0.2871	0.3020448	0.312036	0.320973	0.327885
100000	0.233614	0.28881	0.30386688	0.313896	0.322913	0.329892

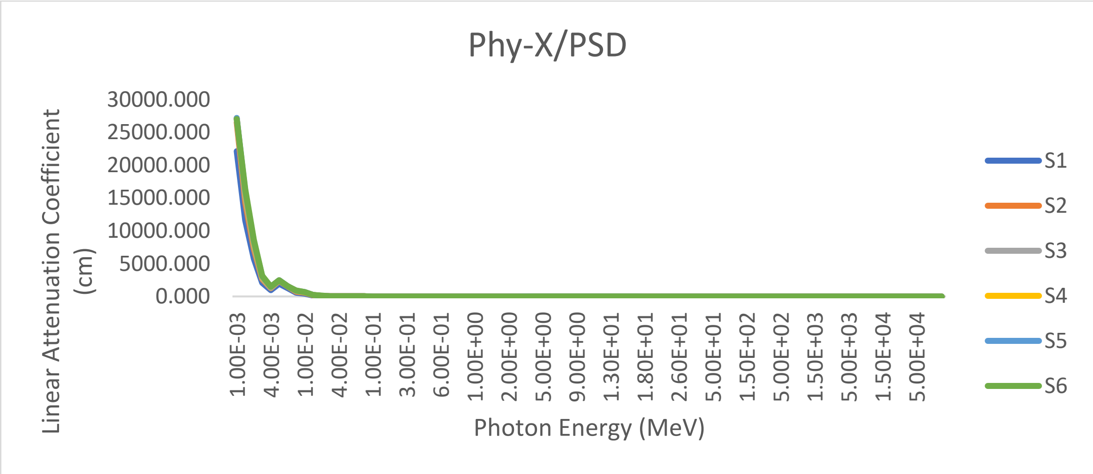

Figure 4: The Graph of Mass Attenuation Coefficient Versus Photon Energy from Phy-X/PSD Simulation

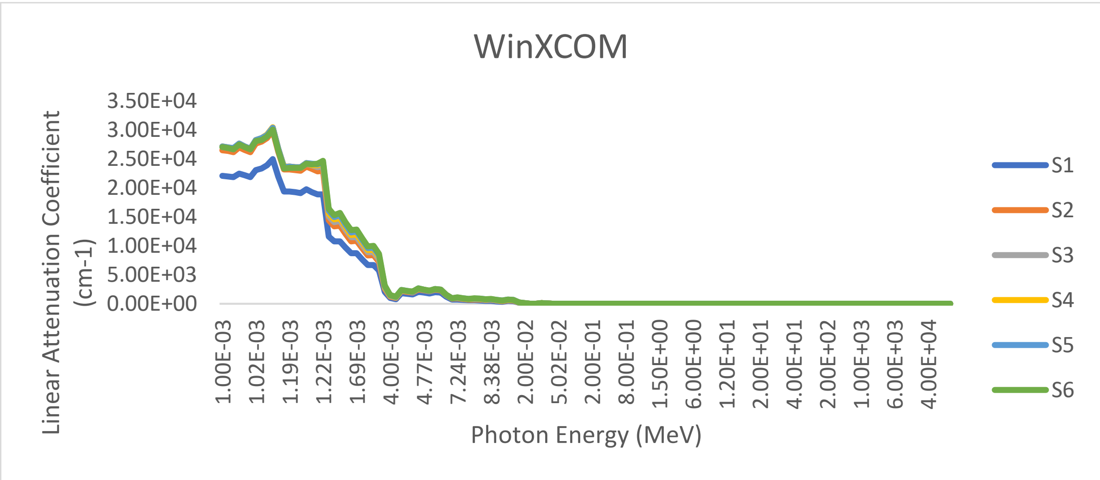

Figure 5: The Graph of Mass Attenuation Coefficient Versus Photon Energy from WinXCOM Simulation

Figures 4 and 5, shows that photon interactions with matter are most significant at low energies, where the highest linear attenuation occur. Different processes dominate at various energy levels: the photoelectric effect at low energies (< 0.1 MeV), Compton scattering at medium energies (above 0.1-1.0 MeV), and the pair production at high energy (1.022 MeV). These interactions influence the LAC values which vary with the photon energy and glass composition.

The LAC values decreased gradually and stabilized above 0.02 MeV, with no significant change observed. The results highlight the impact of gadolinium oxide on the photon resistance of the glass samples. The LAC of the glass samples were influenced by the gadolinium oxide content, with the S6 sample (having highest gadolinium oxide concentration and density) exhibiting the highest LAC values across all photon energies.

Half Value Layer (HVL)

Figures 6 and 7 present the variation of the half-value layer (HVL) as a function of photon energy of the pure and gadolinium doped zinc borotellurite glasses. The Figure 6 was generated from theoretical data obtained from Phy-x/PSD and Figure 7 was derived from WinXCOM calculations. In both datasets, the general trends are consistent, confirming the reliability of the computational approaches in predicting photon attenuation parameters.

Half value layer (HVL) is the measure of the value of sample thickness required to reduce radiation intensity to half its original value (Umeh *et al.*, 2021). Lower HVL values indicate better gamma-ray shielding performance, meaning the material can effectively attenuate more photons (Teresa *et al*., 2021). For Phy-X/PSD data of HVL was obtained directly from software while HVL for WinXCom was calculated from

LAC values using Equation 2. The results obtained from PhyX/PSD and WinXCom were analyzed and then plotted against the respective photon energy as shown in Figure 5 and Figure 6. At a low energy region, which is at 0.001 MeV to 0.04 MeV for both Phy-X and WinXCom, the HVL value is infinitesimal. A rapid increment is observed at 0.04 MeV to 8.0 MeV for both Phy-X/PSD and XCOM. Also, it is observed that on the significantly steep increase there is discontinuation on the graph which indicates the K-absorption edge of heavy elements in the sample that is Gd and Te.

The HVL value starts to decrease and then remains almost constant at 8.0 MeV to 50000 MeV for Phy-X/PSD and 8.0 MeV to 40000 MeV. For WinXCom. In addition, HVL of these samples varies in order as S1 > S2 > S3 > S4 > S5 > S6. This can be ascribed to the increasing concentration of Gd_2O_3 dopant. When 1% to 5% of $0.49TeO_2$, $0.21B_2O_3$ and 0.30ZnO compound is been substituted with Gd_2O_3, the sample become denser. Since LAC varies linearly with density, and HVL varies inversely with LAC, An increase in density will lead to reduction in HVL (Sayyed, 2021). From Figure 5 and Figure 6, it can be deduce that the best sample with lowest HVL is the sample with S6.

Comparing the WinXCOM and Phy/PSD results, the overall shape and relative positioning of the curves are in good agreement with only minor variations in absolute HVL values. This small discrepancies could arise from differences could arise from differences in database cross section parameter. However, both methods clearly show that increasing Gd_2O_3 content systematically improves the gamma-ray shielding performance of the glass by lowering HVL across all energies.

The consistently lower HVL values for Gd containing samples confirm that Gd_2O_3 doping enhances photon attenuation through its high Z contribution, making the glass more effective as a shielding material. The correlation between HVL and composition also supports potential tunability of shielding properties by adjusting the Gd_2O_3 mole fraction.

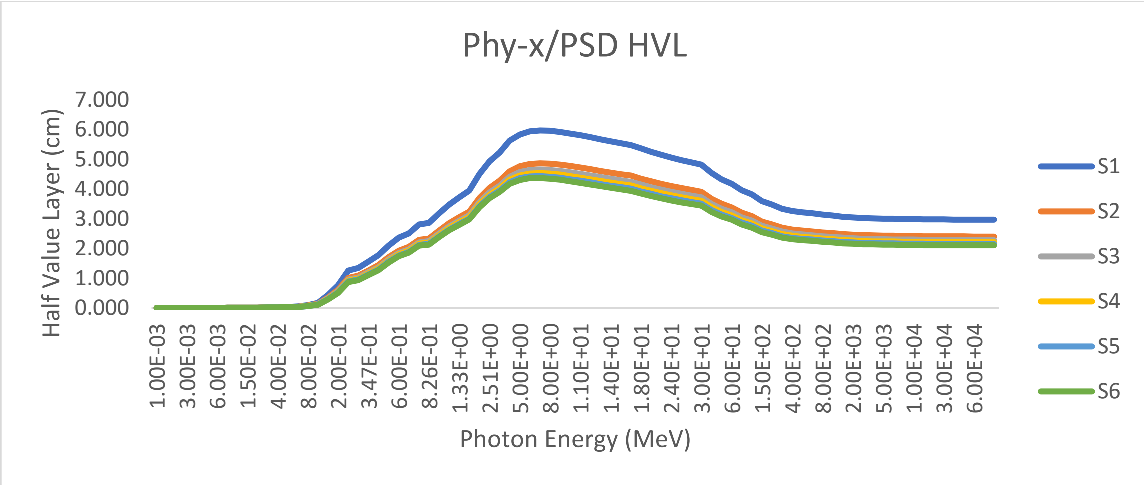

Figure 6: The Graphical Representation of HVL Value in Relation to Photon Energy for Various Glass Composition

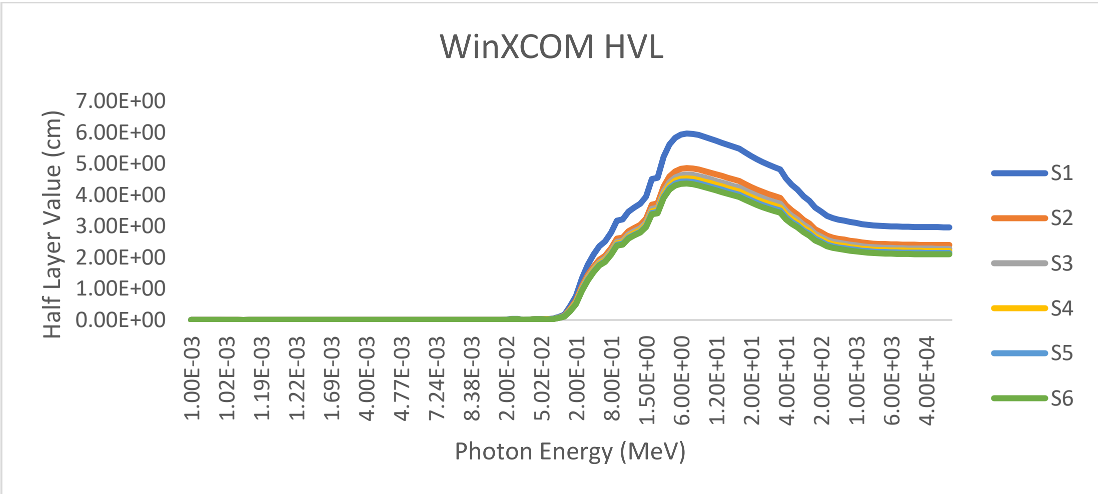

Figure 7: The Graphical Representation of HVL Value in Relation to Photon Energy for Various Glass Composition

Mean Free Path

The average distance of two consecutive collusions is represented by the value of mean free path (MFP) (Alorin *et al.*, 2023). A shorter MFP, indicates more frequent photon interactions, resulting in greater energy absorption and reduced photon transmission. MFP depends on factors such as density, atomic number, and elemental composition. With increasing photon energy, MFP increases, consistent with the decrease in MAC and LAC at higher energies. Figures 8 and 9 shows the bar graph of MFP for at gamma energy of 0.662 MeV, 1.173 MeV and 1.332 MeV. It clear that the MFP value increases as gamma energy value increases for all the glass samples.

Increase G2O3 concentration reduces in MFP across all energies. At 0.662 MeV, S6 achieves MFP = 2.679 cm (Phy-X), representing a 13% reduction relative to S1, quantifying the practical benefit in term of reduce penetration depth. This reduction is attributable to both the increased electron density arising from Gd (Z = 64) and the monotonically increasing bulk density from 3.690 to 4.896 g/cm^3 across the S1–S6 series. S6 exhibits the lowest MFP among all investigated compositions, confirming its superiority for gamma-ray attenuation.

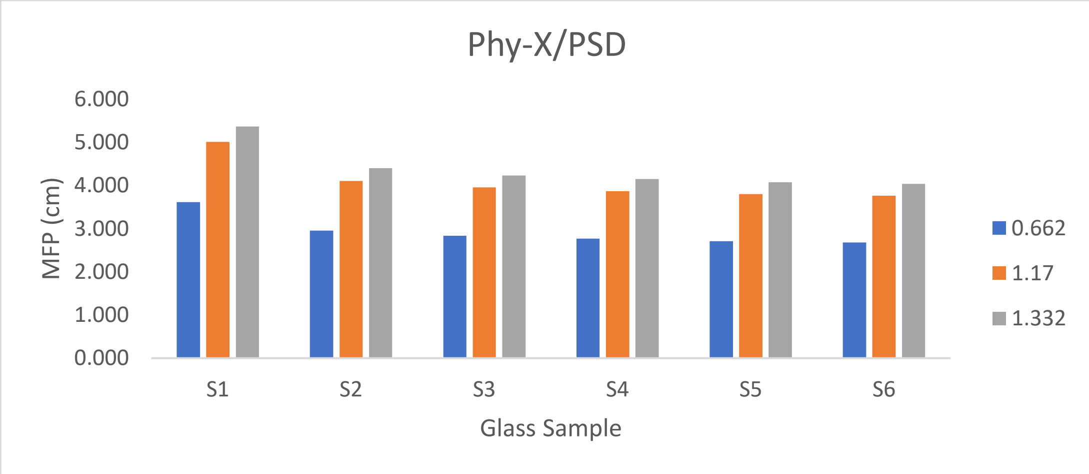

Figure 8: Graph of Mean Free Path Versus Glass Sample

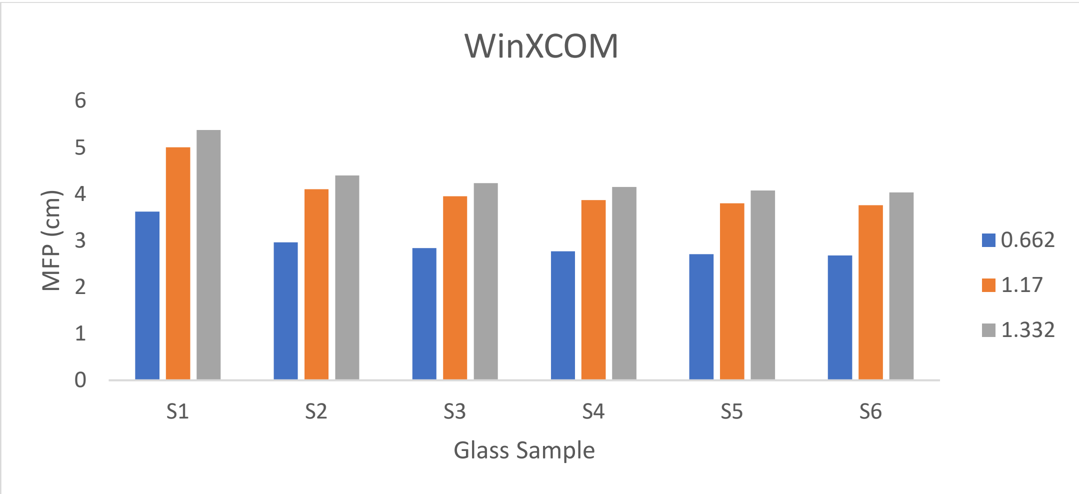

Figure 9: Graph of Mean Free Path Versus Glass Sample

Effective Atomic Number

One of the most promising shielding parameters for determining material's ability to attenuate gamma radiation is effective atomic number (Z_{eff}). Higher value of Z_{eff} of a given composition indicates a greater number of electrons per atom. In practical applications, a high Z_{eff} value desirable in a good radiation shielding glass. For gadolinium-doped zinc borotellurite glass to be suitable for gamma ray shielding, it must possess a high Z_{eff}. Sample S6 having composition 5mol% of G_d2O_3 has the highest Z_{eff}, compared to the rest of the considered glass samples. This makes sample S6, the best composition of the proposed glass as shown in Table 9 and Table 10. Also, our results revealed that as the gamma energy increases, the Z_{eff} decreases. By implication, high gamma energy, lead to low Z_{eff}, photons less likely to be absorbed by the target material.

In general our result reveal that materials with higher molecular mass and density tend to exhibit enhanced shielding properties, provided they have the same elemental composition.

Table 9: Calculated Effective Atomic Number of Pure and Gd-doped Borotellurite Glassusing Phy-X/PSD

Photon Energy (MeV)	S1	S2	S3	S4	S5	S6
0.662	17.65	17.95	18.24	18.53	18.82	19.10
1.17	17.04	17.29	17.54	17.79	18.03	18.27
1.332	17.01	17.26	17.51	17.75	17.99	18.22

Table 10: Calculated Effective Atomic Number of Pure and Gd-doped Borotellurite Glass using WinXCOM

Photon Energy (MeV)	S1	S2	S3	S4	S5	S6
0.662	17.65	17.95	18.25	18.53	18.80	18.98
1.17	17.06	17.31	17.58	17.81	18.05	18.20
1.332	17.01	17.27	17.53	17.75	17.98	18.13

Comparison of Radiation Shielding Properties: 5% Gd_2O_3 Doped Zinc Borotellurite Glass (S6) and Other Materials

Table 11, presents a comparison of S6 (containing 5% Gd_2O_3) obtained from both Phy-X/PSD and WinXCOM, and various proposed radiation shielding materials. Our results show that for a specific glass composition, increasing the concentration of higher molecular weight molecules by decreasing or replacing lower molecular weight molecules leads to an increase in density and subsequently enhances the MAC value. However, a comparison of the MAC values and densities of different materials in Table 3 reveals that the material with the higher MAC value cannot be predicted solely based on its density.

For instance, the borotellurite glass by (Çağlar *et al*., 2021) has a density of 4.26 g/cm³ and MAC values of 0.07625, 0.05329, and 0.0508 cm²/g at 0.662, 1.17, and 1.332 MeV, respectively. In comparison, our sample (S6) has a higher density of 4.896 g/cm³ and MAC values of 0.07623, 0.05423, and 0.05062 cm²/g at the same energies. On the other hand, lead has a much higher density of 11.43 g/cm³ but MAC values of 0.0618 and 0.0562 cm²/g at 1.17 and 1.332 MeV, which are not necessarily higher than those of the glass samples. Meanwhile, the S2 glass sample by (Sallam *et al.*, 2021) has a lower density of 2.5174 g/cm³ but MAC values of 0.0757, 0.0576, and 0.054 cm²/g, which are comparable to those of the other glass samples.

These findings suggest that while density plays a role in determining MAC values, it is not the sole determining factor. The MAC value is influenced by a complex interplay of factors, including the atomic number, elemental composition, and material-specific properties. Therefore, when evaluating the radiation shielding properties of different materials, it is essential to consider their unique compositions and properties rather than relying solely on density as a predictive factor.

Though, lead sodium lithium borosilicate (Salama *et al.*, 2019) has higher MAC, the toxicity and opacity of lead-based materials pose significant limitations. Lead's harmful effects on humans' health and the environment, combined with unsuitability line of sight applications, make lead free 5% Gd-doped zinc boretellurite glass, (S6) a more attractive option gamma radiation shielding especially at 0.662 MeV.

Table 11: Comparison of Mean Attenuation Coefficient for Proposed Glass Sample and Other Shielding Materials

Glass Code	Density (g/cm³)	Mean Attenuation Coefficient Gamma Energy (MeV)			References
		0.662	1.170	1.332	
Borotelluite glass	4.26	0.07625	0.05329	0.0508	(Çağlar *et al.*, 2021)
Lead	11.43		0.0618	0.0562	(Klingberg, 2009)
Lead sodium lithium borosilicate glass	3.91	0.082		0.053	(Salama *et al.*, 2019)
S2	2.5174	0.0757	0.0576	0.054	(Sallam *et al.*, 2021)
S6 Phy-X/PSD	4.896	0.07623	0.05423	0.05062	This work
S6 WinXCOM	4.896	0.07620	0.05430	0.05062	This work

Table 12 presents a comparison of the Half-Value Layer (HVL) results for sample S6, containing 5% Gd_2O_3, obtained from Phy-X and WinXCom, with other known radiation shielding materials at gamma energies of 0.662 MeV, 1.173 MeV, and 1.332 MeV. Notably, the proposed sample S6 exhibits the lowest HVL compared to lead zinc borate glass (El-Kameesy *et al.,* 2013) , Neck glass (Sallam et al., 2025) and 5CeBTe (Rusni *et al.*, 2024). This observation is consistent with the general trend that, for material with the same or different chemical compositions, the one with a higher density tends to have a lower HVL. Since S6 has the highest density among the compared materials, it consequently has the lowest HVL. By implication S6 with the lowest HVL is significant, as it suggests that S6 can effectively attenuate gamma radiation with a thinner layer, making it a promising material for radiation shielding applications. Interestingly, unlike the HVL, the Mass Absorption Coefficient (MAC) did not exhibit a specific tend with different compositions, highlighting the complex relationship between material properties and radiation shielding performance.

Table 12: Comparison of Half Value Layer for Proposed Glass Sample and other Shielding Materials

Glass Code	Density (g/cm³)	Half Value Layer (cm)			Reference
		0.662 (MeV)	1.170 (MeV)	1.332 (MeV)	
Neck Glass	3.4044	2.311	3.455	3.729	(Sallam, Mohamed, Taha, Ahmed, & Eman, 2025)
S3	2.6196	3.425	4.66	4.984	(Sallam, Madbouly, Moussa, & Abdel-Galil, 2021)
Lead zinc borate glass (20% lead)	3.675	2.256	3.207	3.382	(El-Kameesy, El-Ghany, El-Hakam Azooz, & El-Gammmam, 2013)
5CeZBTe	4.69	1.966	2.700	2.889	(RozI, L, & A, 2025)
S6 Phy-X/PSD	4.896	1.857	2.611	2.798	Present work
S6 WinXCOM	4.896	1.858	2.607	2.796	Present work

Table 13 presents a comparison of the Mean Free Path (MFP) of our proposed glass sample S6, containing 5% Gd, with other radiation shielding materials at photon energies of 0.662 MeV, 1.173 MeV, and 1.332 MeV. Notably, sample S6 exhibits the lowest MFP due to its highest density, indicating superior radiation shielding performance. This suggests that our proposed glass sample S6 is a promising material for radiation shielding applications, making it an attractive option for use in environments where radiation protection is critical, such as in medical or industrial settings, and highlighting it's potential as a superior radiation shielding material.

Table 13: Comarison of Half Value Layer for Proposed Glass Sample and Other Shielding Materials

Glass Code	Density (g/cm^3)	Mean Free Path (cm)			References
		0.662 (MeV)	1.170 (MeV)	1.332 (MeV)	
0.4BaSO4	2.87	4.54	6.13	6.55	(Watter, 2025)
Borotellurite glass	4.260	3.077	4.405	4.630	(Çağlar *et al.*, 2021)
Lead zinc borate glass (20% lead)	3.675	3.257	4.630	4.878	(El-Kameesy *et al.*, 2013)
5CeZBTe	4.69	2.836	3.895	4.168	(Rozi *et al.*, 2025)
S6 calculated via Phy-X/PSD	4.896	2.679	3.766	4.037	Present work
S6 calculated Via WinXCOM	4.896	2.680	3.761	4.035	Present work

Table 14 compares the effective atomic number (Z_{eff}) of our sample S6, containing 5% Gd2O3, with various radiation shielding materials, including Ba-Mg-Na-Alumina-Borate, Pb-Na-Li-borosilicate glass (25% Pb), 100 PbO (phr), and 5CeZBTe glasses. Sample S6 exhibits a higher Z_{eff} value, indicating its superior gamma radiation shielding capabilities. With a higher Z_{eff} value, sample S6 can more effectively absorb gamma radiation, making it a superior radiation shielding material compared to the others listed.

Table 14: Comparison of Effective Atomic Number for Proposed Glass Sample and other Shielding Materials

Radiation Shielding Material	Density (g/cm^3)	Effective Atomic Number (Z_{eff})			Reference
		0.662 (MeV)	1.170 (MeV)	1.332 (MeV)	
Ba-Mg-Na-Alumina-Borate		12.06	11.57	11.56	(Singh *et al.*, 2021)
Pb-Na-Li borosilicate glass (25% Pb)	3.91	10.587		9.747	(Salama *et al.*, 2019)
100 PbO (phr)	3.65	6.117	5.534	5.487	(Gamal, et al., 2023)
5CeZBTe	4.69	14.5872	14.711	14.841	(Rozi et al., 2025)
S6 via Phy-X/PSD	4.896	19.10	18.27	18.22	Present work
S6 Via WinXCOM	4.896	18.98	18.20	18.13	Present work

CONCLUSION

This study computationally investigated the gamma-ray radiation shielding properties of a $\{[(TeO_2)_{0.7}(B_2O_3)_{0.3}]_{0.7}[ZnO]_{0.3}\}_{1-x}\{Gd_2O_3\}_x$ glass series (x = 0.00–0.05 mol) using Phy-X/PSD and WinXCOM software. The two platforms yielded closely consistent results, with a maximum inter-software deviation of 0.088%, validating the computational approach.

The superior shielding performance of S6 (5 mol% Gd_2O_3) relative to undoped S1 is mechanistically driven by two coupled effects. First, Gd_2O_3 doping progressively raises the effective atomic number (Z_eff from 17.65 for S1 to 19.10 for S6 at 0.662 MeV), which amplifies the photoelectric cross-section ($\propto Z^4/E^3$) at low to intermediate energies and the pair production cross-section ($\propto Z^2$) above 1.022 MeV. Second, the substitution of lower-Z network formers by the heavier Gd_2O_3 increases bulk density from 3.690 to 4.896 g/cm^3, directly raising the linear attenuation coefficient (LAC = MAC × ρ) and reducing both HVL and MFP. These two mechanisms act in concert: neither density nor atomic number alone is sufficient to explain the observed trends.

The practical significance of these improvements is quantifiable. At 0.662 MeV (^{137}Cs), S6 achieves an HVL of 1.857 cm approximately 21% lower than S1 (2.358 cm), meaning an S6 shielding panel can be made one-fifth thinner than an equivalent S1 panel for the same dose reduction. Its MFP of 2.679 cm implies that a 5 cm S6 panel attenuates approximately 84% of incident photons at this energy, a level of protection requiring 26% more material thickness if S1 were used instead. These gains are relevant to space constrained applications such as diagnostic radiology windows and nuclear medicine facility shielding.

The results also indicate that composition can be tuned to application: S6 is optimal for industrial and medical environments involving higher-energy gamma sources, while intermediate compositions (S2–S3) may be preferable where optical clarity or reduced panel weight is a priority, and S1 retains an advantage for low-energy X-ray shielding below 0.01 MeV where its MAC is highest.

All findings in this study are based on theoretical calculations assuming homogeneous glass mixtures. While this assumption is validated by the inter-software agreement, experimental synthesis and direct measurement of the predicted compositions are necessary before deployment, as real glass microstructure and phase distribution may locally modify attenuation properties. Future work should explore Gd_2O_3 concentrations beyond 5 mol%, other non-toxic high-Z dopants, and experimental verification of the computational predictions reported here

REFERENCES

Al-Hadeethi, Y., Ahmad, M., Al-Heniti, S., Sayyed, M., & Rammah, Y. (2020). Rare Earth Co-doped Tellurite Glass Ceramics: Potential Use in Optical and Radiation Shielding Applications. *Ceramics International, 46*(11), 19198-19208.

Alorin, D. A., Elsafi, M., Almuqrin, A. H., Yasmin, S., & Sayyed, M. I. (2023). Study the Radiation Attenuation Properties of MgO/BariteComposite Ceramics for Photon

Shielding Application. *Digest Journal of Nanomaterials and Biostructures* , *18*(3), 1125-1137.

ARPANSA. (2022). Gamma radiation. Radiation Protection and Nuclear Safety Agency. Australian. doi:: https://www.arpansa.gov.au/understanding-radiation/what-is-radiation/ionising-radiation/gamma-radiation

Azuraida, A. (2018). Structural, Optical and Shielding Properties of Bi2O3/BaO-B2O3-TeO2 Doped CeO2 Glass System.

Berger, M., & Hubbell, J. H. (1987). XCOM: Photon cross sections on a personal computer. National Bureau of Standards. Washington, DC (USA). *Center for Radiation Research*, 1-27.

Çağlar, I., Cengiz, G. B., & Bilir, G. (2021). Gamma Radiation Shielding Properties of Some Binary TelluriteGlasses. *Journal of Non-Crystalline Solids,, 574*. doi: https://doi.org/10.1016/j.jnoncrysol.2021.121139

Callister, W. D., & Rethwisch, D. G. (2011). *Material and Engineering.* Wiley: SI version.

Echeweozo, E. O., Ali, M. S., Nwigwe, G. C., Nady, M., Attalla, M. E., Sherkawy, E.-S., & Abdelmonem, A. M. (2025). Theoretical Evaluation of Radiation Shielding and Particle Interaction Feature of ZnOP2O5 Glass Systems Doped withPbO Nanoparticles. *SOHAG Journal OF SCIENCE, 10*(1), 181-192. doi: https://doi.org/10.21608/sjsci.2025315293.1220

Eevon, C., M, K. H., Z, A., & C, A. (2016). Elastic Properties of TeO2 - ZnO-Gd2O3 GlassesUsing Non-Destructive Ultrasonic Technique. *Chalogenide Letters, 13*(6), 281-289.

Effendy, N., Zaid, M. H., H. Sidek, A. A., Matori, K. A., Mahmoud, K. A., & Sayyed, M. I. (2021). Influence of ZnO to the physical, elastic and gamma radiation shielding properties of the tellurite glass system using MCNP5 simulation code. *Radiation Physics and Chemistry*. doi: https://doi.org/10.1016/j.radphyschem.2021.109665

El-Kameesy, S. Y., El-Ghany, S. A., El-Hakam Azooz, M. A., & El-Gammmam, Y. A. (2013). Shielding Properties of Lead Zinc Borate Glasses. *World Journal of Condensed Matter Physics,* 3(4), 198–202. doi: https://doi.org/10.4236/wjcmp.2013.34033

El-Mallawany, R. (2002). *Tellurite Glasses HANDBOOK.* USA: CRC Press Inc, Boca Raton, FL.

Gamal, R., Salama, E., Hassan, E., El-Nashar, D., Assem, B., & Ehab, M. (2023). Gamma Attenuation and Mechanical Characteristics of a Lead/NBR/SBR Rubber Composite with Black Nanocarbon Reinforcement. *Sustainability, 15*(2165), 1-17. doi: https://doi.org/10.3390/su15032165

Hasnimulyati, L., Hlimah, M. K., Abdul, H. S., Ishak, M., Azuraida, A., & Nazrin, S. N. (2021). Structural Properties of Cerium Oxide Doped Zinc Borotellurite Glass. *Gading Journal of Structural and Technology, 4*(2), 58-65.

Hatice, Y. A. (2024). A Study on the Effect of Addition Li, Na, and K on the Radiation Shielding Capabilities of B2O3-TeO2-ZnO-PbF2-Er2O3 Glass Structure. *Journal of Science and Engineering, 24*, 789-797.

Jamal, N., Natasha, M., Aida, N., & Amin, B. (2020). Tungsten-based Material as a Promising New Lead-free Gamma Radiation Shielding Material in Nuclear Medicine. *Physica Medica, 78*, 48-57. doi: https://doi.org/10.1016/j.ejmp.2020.08.017

Kavaz, E., Ekinci, N., Tekin, H. O., Sayyed, M. I., Aygün, B., & Perişanoğlu, U. ". (2019). Estimation of gamma radiation shielding qualification of newly developed glasses by using WinXCOM and MCNPX code. *Progress in Nuclear Energy, 115*, 12-20. doi: https://doi.org/10.1016/J.PNUCENE.2019.03.029

Klingberg, F. (2009). Cability to Determine Shielding Around Radioactive Substances using Gamma Ray Spectrometry Diploma Thesis.

Matori, K. A., Sidek, H. A., Zaid, M. H., & Singh, V. P. (2017). Comprehensive study on physical, elastic and shielding properties of lead zinc phosphate glasses. *Journal of NonCrystalline Solids, 457*, 97-103. doi: https://doi.org/10.1016/jncrysol.2016

Roberts, P. B. (2003). Encyclopedia of Food Science and Nutrition. *3390*. doi: https://doi.org/10.1016/B0-12-227055-X/00655-6

Rozi, N. F., L, H., & A, A. (2025). Simulated Radiation Shielding Parameter for Energy 1keV-100GeV of Lead-Freeborotellurite Based Glass for Nuclear Medicine Applications. *Chalcogenide Letter, 22*(1), 57-76.

Rusni, N. A., Hasnimulyati, L., & Azurriada, A. (2004). Theoretical Ionizing Radiation Shielding Parameters of Thulium Doped Zinc Borotellurite Glass. *E3S web Conferences, 481*, 1-16. doi: https://doi.org/10.1051/e3sconf/20248103009

Rusni, N. M., Azuraida, A., Wan, Y. W., Nor, A. A.-M., & Nurazlin, A. (2024). Mechanical Properties of Thiulium-doped Bismuth Borotellurite Glass via Nanoindentation for Lead-FreeRadiation Shielding Application. *Journal of Integrated Engineering, 16*(6), 206-215.

Saheb, M. S., Vijay, R., Rao, P. V., Ramesh, P., Chandrakala, B., Prasad, P., & Raju, G. (2018). *Result Physics, 11*, 780-786.

Salama, E., Abeer, M., & G, M. Y. (2019). Gamma Radiation and Neutron Shielding Properties of Transparent Alkali Borosilicate Glass Containing Lead. *Journal of Physics and Chemistry of Solid, 131*, 139-147.

Sallam, O. I., Mohamed, A. K., Taha, A. A., Ahmed, A. E.-S., & Eman, Y. F. (2025). Determination of Some Optical, Structural and Radiation Shielding Properties of Waste glass From Cathode Ray Tube. *Silicon*, 1-14.

Sallam, O., Madbouly, A. M., Moussa, N. L., & Abdel-Galil, A. (2021). Impact of Radiation on CoO-doped Borate Glass: Lead-free Radiation Shielding. *Applied Physics A: Material Science & Processing, 128*(70), 69-86.

Sayyed, M. I. (2021). Experimental and Theoretical Study of Radiation Shielding Features of CaO-K2O-Na2O-P2o5 Glass

Systems. *Materials, 14*(14). doi: https://doi.org/10.3390/ma14143772

Singh, S., Kaur, R., Rani, S., Sidhu, B., & S. (2021). Physical, structural and nuclear radiation shielding behaviour of xBaO(0.30x)MgO0.10Na2O0.10Al2O30.50B2O3 glass matrix. *Materials Chemistry and Physics, 276*, 125415. doi: https://doi.org/10.1016/j.matchemphys.2021.125415

Teresa, E. P., Naseer, K. A., Marimuthu, K., Alorani, H., Aljawhara, H. A., & Sayyed, M. I. (2021). Optical Properties and Radiation Shielding Studies of Europium Doped Modifier Reliant Multi Former Glasses. *Optik-International Journal for Light and Electronic Optics*, 1-13. doi: https://doi.org/10.1016/j.radphyschem.2o21.109741

Udiba, U. U., Ekom, R. A., & Ekpo, E. A. (2019). Soil Lead Concentrations in Dareta Village, Zamfara, Nigera. *Journal of Health & Pollution, 9*(23). doi: https://doi.org/10.5696/2156-9614-9.23.190910

Umeh, C. D., Agwu, K. K., Okoye, C. M., Ahia, C. C., & Ikegbu, G. O. (2021). Characterization of the radiation shielding properties of fired lead sample for X-ray shielding applications. *Progress in Nuclear Energy, 137*, 103765. doi: https://doi.org/10.1016/j.pnucene.2021.103765

Watter, H. (2025). AComperehensive Study on the Effect of BaSO4 on Gamma-Ray Shielding Properties of B2O3-CaO-Na2O-SiO2 Glass System, a Comparative Evaluation Using Phy-X/PSD and XMuDat Program. *University of Thi-Qar Journal of Science (UTJsci), 12*(1), 133-140.